Available online at www.sciencedirect.com

ScienceDirect

Procedia Structural Integrity 8 (2018) 462–473

Structural Integrity Procedia

www.elsevier.com/locate/procedia

AIAS 2017 International Conference on Stress Analysis, AIAS 2017, 6-9 September 2017, Pisa, Italy

Commissioning of a Novel Test Apparatus for the Identification of the Dynamic Coefficients of Large Tilting Pad Journal Bearings

Forte P.*[a],Ciulli E.[a], Maestrale F.[b], Nuti M.[b] , Libraschi M.[c]

[a] *Department of Civil and Industrial Engineering, University of Pisa, Largo Lazzarino, 56122 Pisa, Italy*
[b] *AM Testing, Via Padre Eugenio Barsanti 10, Loc. Ospedaletto, 56121 Pisa, Italy*
[c] *BHGE, Via Felice Matteucci 2, 50127 Florence, Italy*

Abstract

This paper describes the commissioning of a novel test bench for the static and dynamic characterization of large tilting pad journal bearings, realized within a collaboration of the Department of Civil and Industrial Engineering of the University of Pisa, BHGE and AM Testing.
The adopted test bench configuration has the test article (TA) floating at the mid-span of a rotor supported by two rolling bearings. The TA is statically loaded vertically upwards by a hydraulic actuator and excited dynamically by two orthogonal hydraulic actuators with multiple frequency sinusoidal forces. The test rig is capable of testing bearings with a diameter from 150 to 300 mm. It includes very complex mechanical, hydraulic, electrical and electronic components, and needs, for the whole plant, about 1 MW of electric power.
The commissioning of the testing system involved several aspects and presented various issues. This work focuses on measuring systems and data acquisition of high-frequency data (forces, accelerations and relative displacements) and on data processing for the identification of the bearing dynamic coefficients. The identification procedure is based on the linearity assumption and the principle of superposition, operating in the frequency domain with the fast Fourier transforms of the applied forces and displacement signals. First results, referred to a 4-pad bearing, are in satisfactory agreement with theoretical ones.

Copyright © 2018 The Authors. Published by Elsevier B.V.
Peer-review under responsibility of the Scientific Committee of AIAS 2017 International Conference on Stress Analysis

* Corresponding author. Tel.: +39-050-2218046; fax: +39-050-2218065.
E-mail address: p.forte@ing.unipi.it

2452-3216 Copyright © 2018 The Authors. Published by Elsevier B.V.
Peer-review under responsibility of the Scientific Committee of AIAS 2017 International Conference on Stress Analysis
10.1016/j.prostr.2017.12.046

Keywords: Tilting pad journal bearings, test bench, experimental identification, dynamic coefficients, turbomachinery

1. Introduction

Tilting pad journal bearings (TPJBs) are commonly used in turbomachines for their stability characteristics at high speed and low load operating conditions.

Assuming linear and synchronous behavior the dynamic characteristics of the bearings can be expressed by stiffness and damping matrices (**K** and **C**), 2x2, which are fundamental in the study of rotor dynamics. Mathematical models are validated and calibrated by comparing the theoretical results with experimental ones obtained on specific test stands by applying dynamic loads (harmonic forces, impulsive or random) to the bearing or to the rotor and measuring their relative relative displacement. For a review on experimental apparata and procedures refer to the work of Dimond et al. (2009). The most common test bench configuration has the test bearing floating at mid-span of a fixed rotor supported by two rolling bearings. The bearing is loaded statically and it is dynamically excited by two independent actuators in two orthogonal directions. Examples of such configured test benches are described by Childs and Hale (1994), Ha and Yang (1999), Wygant et al. (2004), Ikeda et al. (2006), Bang et al. (2010). Less common is the configuration of two identical fixed test bearings that support the rotor free to move more like a real configuration, as adopted by Chatterton et al. (2014) and Dang et al. (2016), although limited to smaller bearing diameters.

Unfortunately the dynamic bearing coefficients are not directly scalable with diameter. That justifies the effort of developing a new test facility for the dynamic characterization of large TPJBs to extend the ranges of test parameters and support the development of products of industrial interest.

At the University of Pisa a new testing platform, unique in Europe for size and power, was designed and set up within a collaboration between the Department of Civil and Industrial Engineering of the University of Pisa, BHGE and AM Testing with Tuscany Region funds. For details of the design process refer to Forte et al. (2016). The test bench commissioning ended in early 2017. This paper illustrates the major features of the test facility and the first experimental results.

Nomenclature

A	stator acceleration component
c	damping coefficient
C	damping matrix
D	relative displacement component
$\boldsymbol{D}$	relative displacement vector
D	relative displacement matrix
F	force component
$\boldsymbol{F}$	force vector
F	force matrix
H	impedance matrix
k	stiffness coefficient
K	stiffness matrix
M	stator mass
Δ	difference
ω	angular frequency
subscripts:	
af	anti-phase
b	bearing
s	stator
f	in-phase
u,v	directions of dynamic actuators

x,y	horizontal and vertical directions

2. The test bench

The test bench is depicted in Fig. 1 with a drawing, where the main groups are indicated, and a picture. Figure 2 presents, on the left, a view of the test plant with the low pressure lubrication system in the background, on the right the mounting of the rotor. The test apparatus main characteristics are summarized in Table 1.

The size of the test bearing brought along various consequences as regards its configuration. The test bearing is floating at the mid-span of the rotor supported by two rolling bearings (Fig. 3). The test bearing is statically loaded vertically upwards by a hydraulic actuator and excited dynamically by two orthogonal hydraulic actuators at 45° with respect to the vertical direction. The actuators are identical and can operate independently or simultaneously. An anti-roll arm relieves the actuators, from the duty of limiting the rotation of the bearing casing (stator) around the longitudinal axis (Z) and of counteracting the bearing hydrodynamic friction. A power of about 1 MW is necessary for the electric motor driving the rotor and for the auxiliary plants. All the involved mechanical, hydraulic, electric and electronic systems are quite complex because they are designed for uncommon, extreme performances.

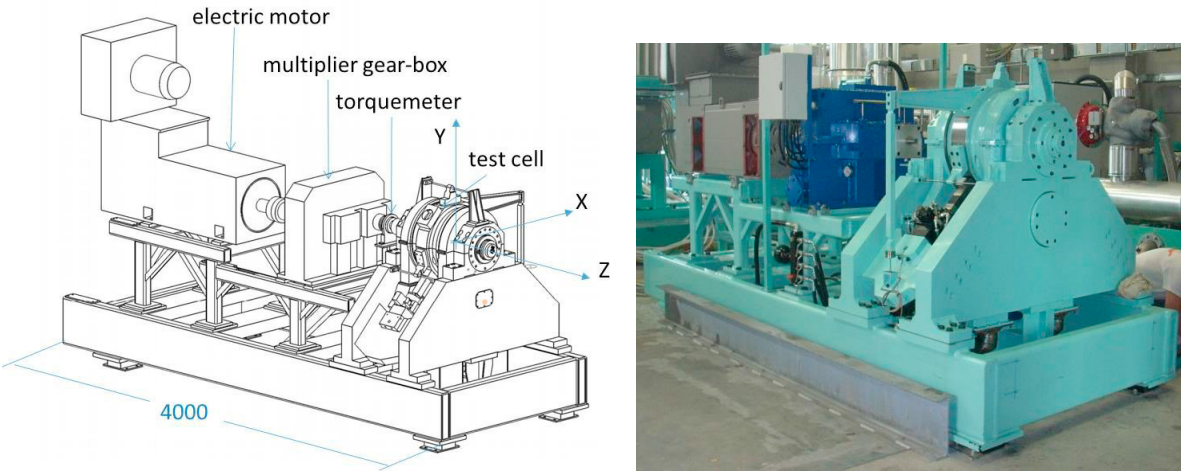

Fig. 1. Drawing and photograph of the test bench.

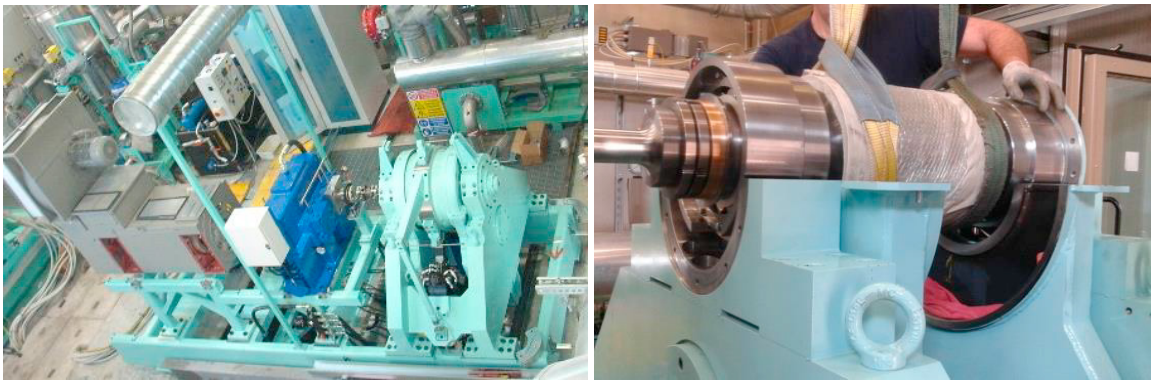

Fig. 2. View of the test plant and picture of rotor mounting.

Table 1. Test bench main characteristics.

Characteristic	Value
Test bearing diameter (mm)	150 - 300
Bearing length/diameter	0.4 - 1
Shaft rotating speed (rpm)	0 – 24000
Peripheral speed (m/s)	0 - 150
Static load (kN)	0 - 270
Dynamic load (kN)	0 - 30
Dynamic load frequency (Hz)	0 - 350
Oil flow rate (l/min)	125 - 1100
Oil input temperature (°C)	30 - 120

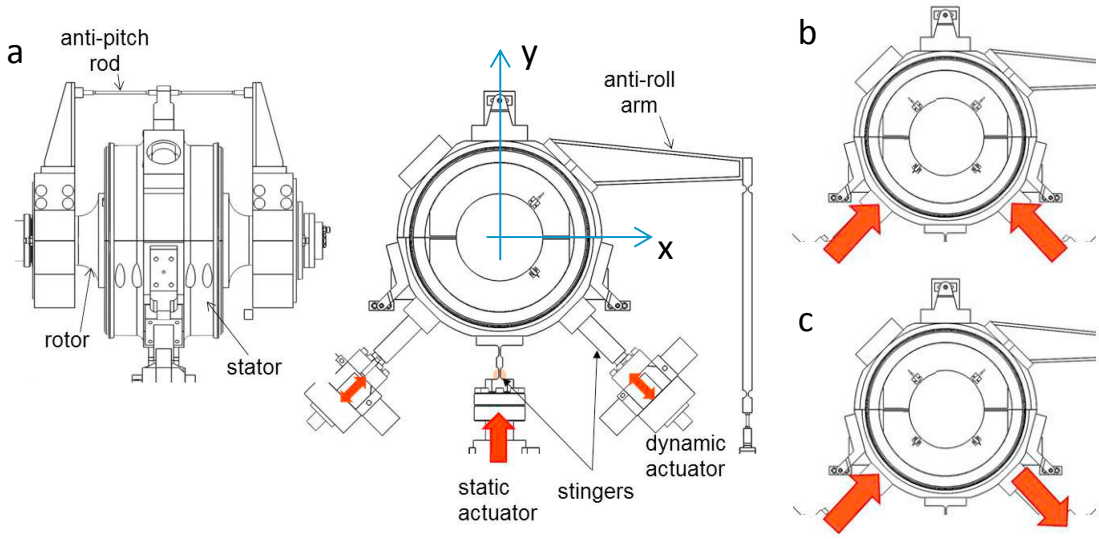

Fig. 3. (a) the loading system; (b) in-phase mode; (c) anti-phase mode.

The bench, including the auxiliary plants, is equipped with about 90 sensors in order to measure relevant quantities (oil temperature, pressure and flow-rate at different points, force, angular speed, relative displacement, acceleration). Focusing on the test cell and on the quantities necessary for the identification of the bearing dynamic coefficients, the relevant sensors are load cells measuring the significant forces applied on the bearing casing (stator), proximity sensors measuring the relative displacement between the stator and the rotor, and accelerometers measuring the stator acceleration.

Figure 4a shows the position of the load cells. Two tri-axial load cells (Fig. 4b), with 40 kN full-scale, are located between the dynamic actuators and the stator; one uniaxial load cell, with 300 kN full-scale, in series with a stinger instrumented with strain-gauges, to measure the axial and the tangential force respectively, is located between the static actuator and the stator and one uniaxial load cell, with 1 kN full-scale, is located between the anti-roll arm rod and the bench frame.

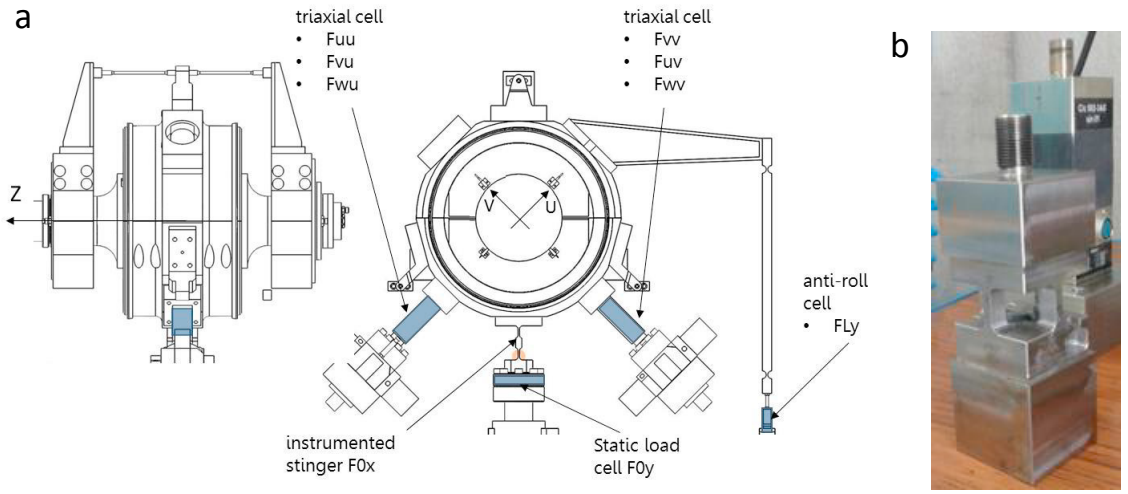

Fig. 4. (a) location of the load sensors; (b) picture of triaxial cell.

Figure 5 shows the position of the proximity sensors. A total of eight proximity sensors, with a sensitivity of about 0.1 μm, were located in the direction of the dynamic actuators, distributed on two planes perpendicular to the rotor axis. Four of them are more accurate but have a limited measuring range (800 μm), so they are more suitable for measuring dynamic displacement. The others are less accurate but have a wider measuring range (2000 μm), so they are more suitable for measuring the bearing clearance.

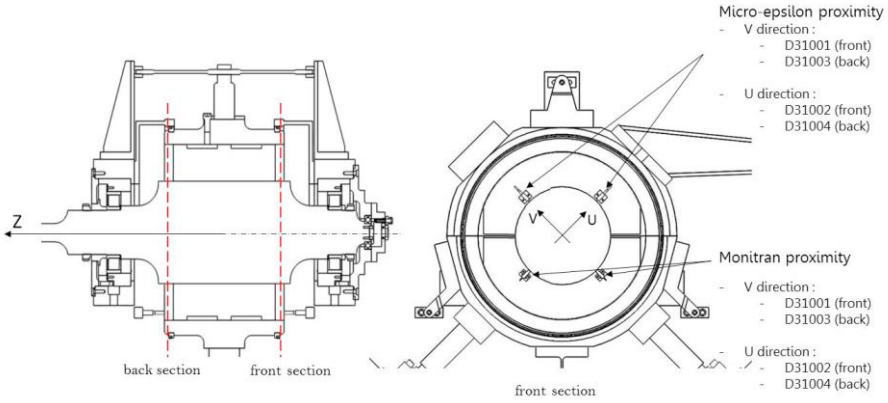

Fig. 5. Location of the proximity sensors.

Figure 6 shows the position of the accelerometers. A total of four uniaxial accelerometers were located in the direction of the dynamic actuators, distributed on two planes perpendicular to the rotor axis.

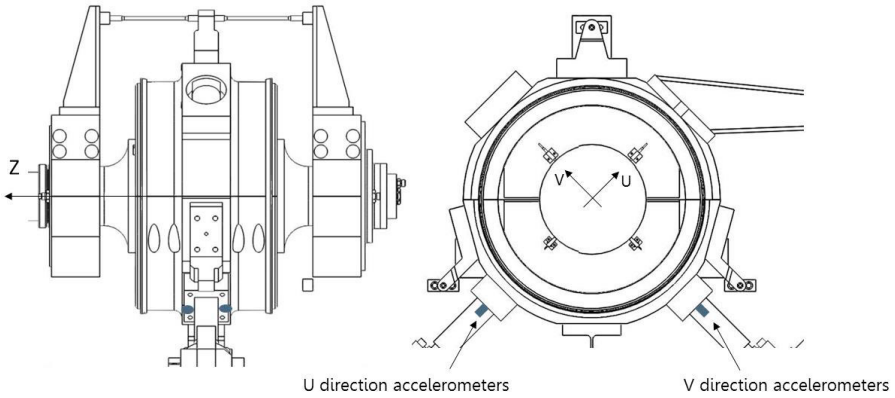

Fig. 6. Location of the accelerometers.

The test management consists in the definition and control of the operating conditions, data acquisition and recording from a large quantity of sensors, requiring complex HW and SW systems. A National Instruments PXI System is devoted to the acquisition of high frequency signals, a CompactRIO platform to the acquisition of low frequency signals. High-frequency data (about 30 signals) are sampled at 100 kHz, low frequency data (about 60 signals) at 1 Hz.

3. The test procedure

The test system is used mainly for two types of tests: the bump test for determining the actual bearing clearance, and the test for the identification of the bearing dynamic coefficients. This paper will focus on the second more demanding type of test even though the first one is complementary for the characterization of the bearing.

Each identification test is characterized by a point of steady state operation, defined by the shaft rotation speed, the static load and the lubricating oil flow rate and inlet temperature. When the steady state conditions are reached, the dynamic actuators impose single or multiple frequency (up to 5) sinusoidal forces in the frequency range of interest, typically below and just above the synchronous frequency, avoiding harmonics and test bench resonances. The results obtained in multi-tone test and corresponding single tone tests, once the control system was tuned, differed less than the measurement error while the time of testing and data processing procedure was significantly reduced. Therefore after a few single tone tests, the multi-tone test was adopted as a standard.

The displacement amplitude must be sufficiently small to avoid the effects of non-linearity in the dynamic behavior of the bearing but sufficiently great with respect to the uncertainty of measurement. A few commissioning trials indicated that 4 kN was the most convenient force amplitude to obtain the appropriate displacement (see section 4). For the identification of the dynamic coefficients, with the assumption of linearity, two tests with linearly independent excitations are required for each excitation frequency, as indicated by Childs and Hale (1994). The actuators typically operate simultaneously in-phase or anti-phase (Fig. 3b and 3c)with the same amplitude imposing to the stator an approximately rectilinear orbit in the vertical or horizontal direction respectively.

The high frequency sensor data are sampled for 1 s at a sufficiently high frequency (100 kHz), and frequency transformed. In particular, such a sampling frequency was adopted in order to get an accurate measure of the rotational speed. The Fourier transform of the force and displacement signals is the input data for the identification process of the dynamic coefficients. Thirty identical tests are repeated in rapid succession and the coefficients averaged to decrease the effect of random errors on the sensor signals.

4. Data processing

The acquired data are processed off-line in order to calculate the bearing dynamic coefficients by purposely developed software codes in Matlab® ambient according to the following analytical steps.

Assuming a linear behavior around the steady state, the bearing reaction on the rotor can be expressed in the frequency domain, as

$$\boldsymbol{F_b} = \mathbf{H}\boldsymbol{D} \tag{1}$$

where $\boldsymbol{F_b}$ is the vector of the horizontal and vertical force components, $\boldsymbol{D}$ that of the two relative displacement components, and **H** is a complex 2x2 matrix representing the bearing frequency response, called by some authors, e.g. Dimond et al. (2011), mechanical impedance. All terms depend on angular frequency, ω.
Equation 1 can be expanded into Eq. 2

$$\begin{bmatrix} F_{bx} \\ F_{by} \end{bmatrix} = \begin{bmatrix} H_{xx} & H_{xy} \\ H_{yx} & H_{yy} \end{bmatrix} \begin{bmatrix} D_x \\ D_y \end{bmatrix} \tag{2}$$

In order to determine the four unknown components of **H** two tests with linearly independent excitations must be carried out, in this case in-phase (*f*) and anti-phase (*af*), obtaining

$$\begin{bmatrix} F_{\mathrm{b}xf} & F_{\mathrm{b}xaf} \\ F_{\mathrm{b}yf} & F_{\mathrm{b}yaf} \end{bmatrix} = \begin{bmatrix} H_{xx} & H_{xy} \\ H_{yx} & H_{yy} \end{bmatrix} \begin{bmatrix} D_{xf} & D_{xaf} \\ D_{yf} & D_{yaf} \end{bmatrix} \tag{3}$$

The relative displacements are measured by the proximity sensors in the direction of the dynamic actuators. Therefore they must be projected and composed in the x and y directions, and fast Fourier transformed.
As for the bearing film force components they are obtained, subtracting the stator inertia from the forces applied to the stator, by the equilibrium equation

$$\begin{bmatrix} F_{\mathrm{b}xf} & F_{\mathrm{b}xaf} \\ F_{\mathrm{b}yf} & F_{\mathrm{b}yaf} \end{bmatrix} = \begin{bmatrix} F_{\mathrm{s}xf} & F_{\mathrm{s}xaf} \\ F_{syf} & F_{syaf} \end{bmatrix} - M \begin{bmatrix} A_{xf} & A_{xaf} \\ A_{yf} & A_{yaf} \end{bmatrix} \tag{4}$$

The first matrix on the right side of Eq. 4 is made by the resultant components of the forces applied to the stator, obtained by measurement in the directions of the force sensors, projection and composition in the x and y directions, and fast Fourier transform (FFT). *M* is the mass of the stator that can be calculated from CAD or measured. The second matrix on the right side is made by the components of the stator acceleration, obtained by measurement in the directions of the accelerometers, by projection and composition in the *x* and *y* directions, and by FFT.
The terms of **H** are then determined, from Equation 3, by the matrix operation

$$\mathbf{H}=\mathbf{F_b}\,\mathbf{D}^{-1} \tag{5}$$

where $\mathbf{F_b}$ and **D** are the 2x2 matrices of bearing force and relative displacement respectively. Thus, the stiffness and damping matrices **K** and **C** can be obtained, as function of ω, by separating the real and imaginary parts of **H**, considering that

$$\mathbf{H} = \mathbf{K} + \mathbf{i}\omega\mathbf{C} \tag{6}$$

In the multi-tone test force and displacement signals are obtained for up to five excitation frequencies. The FFT allows the extraction of force and displacement components at single frequencies and thus, following the procedure described above, the corresponding stiffness and damping matrices are obtained as function of frequency. The synchronous values of the coefficients are finally calculated by interpolation from the data of the various frequencies. That can be done for different rotational speeds as well as for other operating parameters.

5. Commissioning results

The commissioning results reported here are related to a 4-pad TPJB, in the load between pad configuration (Fig. 7). The bearing had a 280 mm diameter and a clearance around 400 μm.

Fig. 7. 4-pad TPJB used for commissioning tests.

Commissioning tests were carried out at different rotating speeds (from 1000 rpm to 6100 rpm) and two static loads (58 kN and 92 kN), oil flow rate from 140 l/min to 160 l/min and inlet temperature from 40°C to 60°C. The dynamic load amplitude was set to 4 kN after some preliminary sensitivity tests (at 40 Hz) that indicated it as the most appropriate value (Tab. 2).

Table 2. Sensitivity to dynamic force amplitude.

Force amplitude (kN)	Δ_{max} k_{xx} (%)	Δ_{max} k_{yy} (%)	Δ_{max} c_{xx} (%)	Δ_{max} c_{yy} (%)
2.5-8	<2%	<5%	<3%	<2%

Figure 8 shows an example of the acquired force and displacement signals measured in the axial direction of the actuators in the in-phase and anti-phase tests for a single tone test. The force signal is rather neat while the displacement signal is more noisy, containing also higher harmonics.

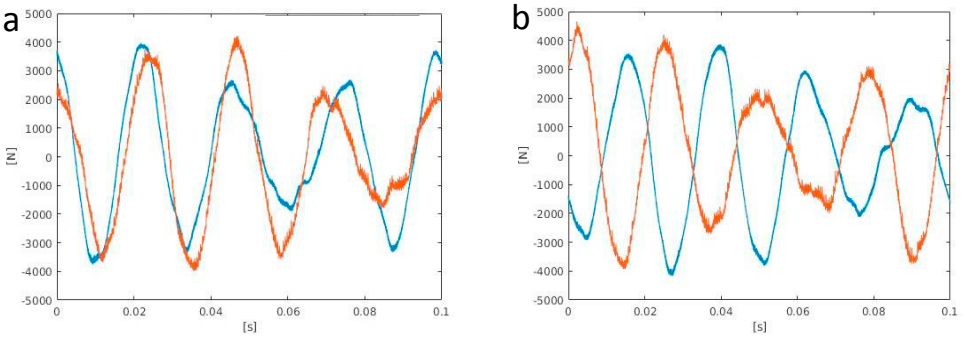

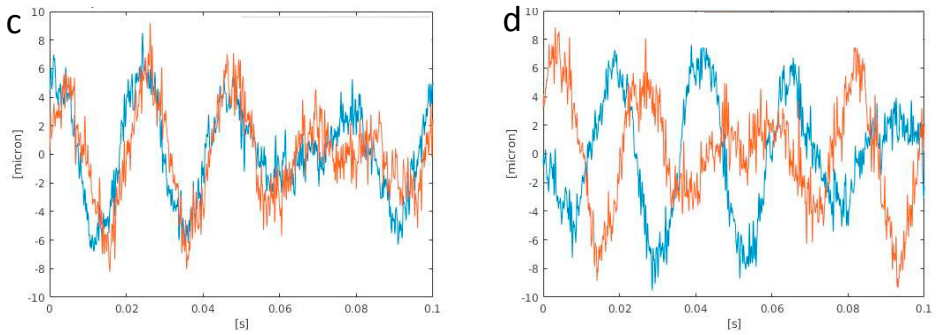

Fig. 8. (a) dynamic actuators in-phase forces; (b) dynamic actuators anti-phase forces; (c) in-phase measured displacements; (d) anti-phase measure displacements; at 3000 rpm, 58 kN static load, 4 kN dynamic load, 40 Hz excitation frequency.

For the same case, Fig. 9 shows the force and displacement signals projected and combined in the vertical and horizontal directions, in the in-phase and anti-phase tests. It is noteworthy that in the first case the dynamic load is mainly vertical with a horizontal minor component while in the second case the opposite occurs. In addition one can notice that the minor component has a different number of cycles (5 instead of 4) in 0.1 s. Such a component is actually due to the synchronous dynamic load generated by rotor unbalance. The synchronous component is more evident in the FFT of the signal (Fig. 10).

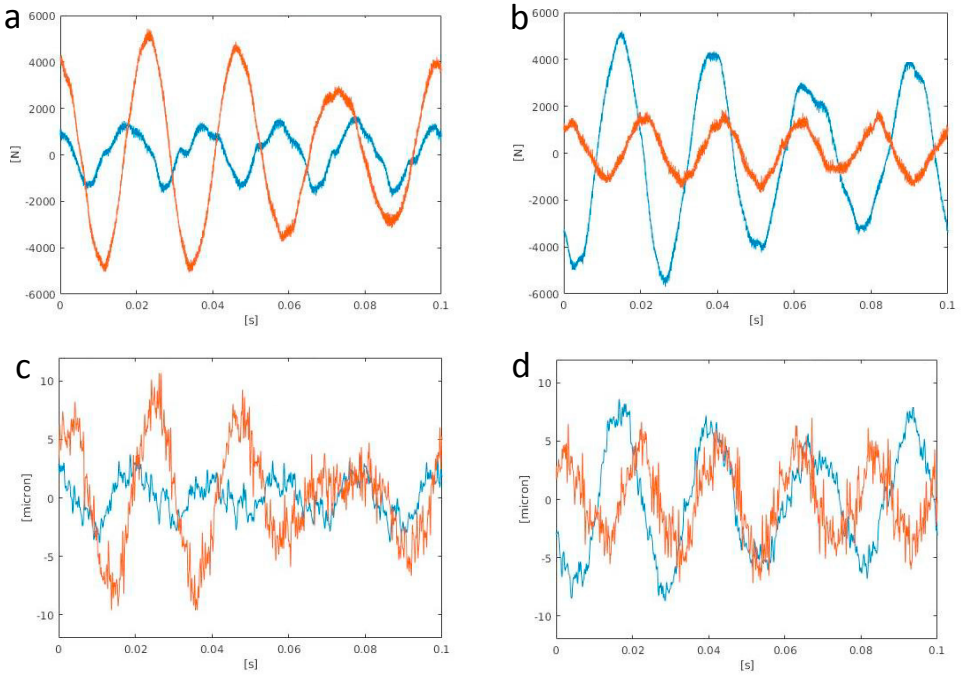

Fig. 9. (a) vertical (red) and horizontal (blue) forces in-phase test; (b) vertical (red) and horizontal (blue) forces anti-phase test; (c) vertical (red) and horizontal (blue) displacements in-phase test; (d)) vertical (red) and horizontal (blue) displacements anti-phase test; at 3000 rpm, 58 kN static load, 4 kN dynamic load, 40 Hz excitation frequency.

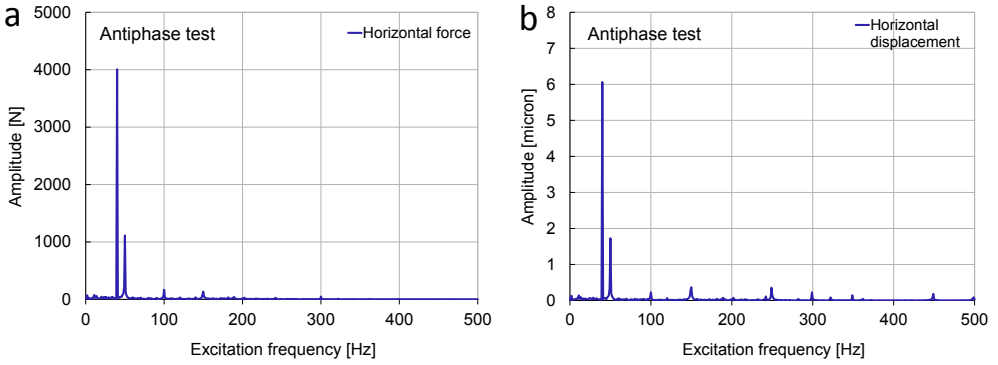

Fig. 10. FFT of (a) horizontal force anti-phase test; (b) horizontal displacement anti-phase test; at 3000 rpm, 58 kN static load, 4 kN dynamic load, 40 Hz excitation frequency.

For the same operating conditions, Fig. 11 shows the vertical and horizontal force and displacement signals in the anti-phase test, in the case of multi-tone excitation. The FFT of the signals (Fig. 12) makes it possible to separate the five different frequency components, evidencing the synchronous component due to rotor unbalance.

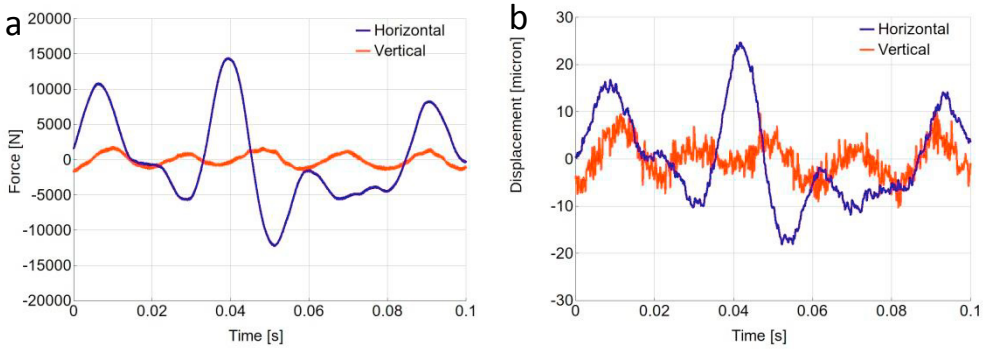

Fig. 11. (a) vertical (red) and horizontal (blue) forces anti-phase test; (b) vertical (red) and horizontal (blue) displacements anti-phase test; at 3000 rpm, 58 kN static load, 4 kN per dynamic load component, 10-22-33-42-58 Hz excitation frequencies.

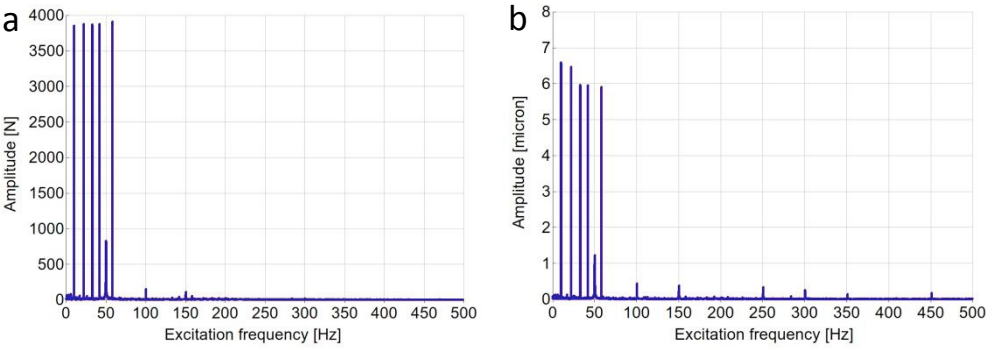

Fig. 12. FFT of (a) horizontal force anti-phase test; (b) horizontal displacement anti-phase test; at 3000 rpm, 58 kN static load, 4 kN per dynamic load component, 10-22-33-42-58 Hz excitation frequencies.

For the same operating conditions, Fig. 13 shows the calculated stiffness and damping coefficients for multi-tone excitation. As expected for TPJBs, the cross-coupled coefficients are much lower than the direct ones. The repeatability of the thirty planned sequential tests was satisfactory with a standard deviation of the coefficients of: less than 1% for the stiffness direct ones, less than 2% for the damping direct ones. The observed non-isotropic behaviour for both stiffness and damping was ascribed to the non-negligible dynamic contribution of the static actuator, not accurately measured, that suggested an upgrade of the static load cell conditioner.

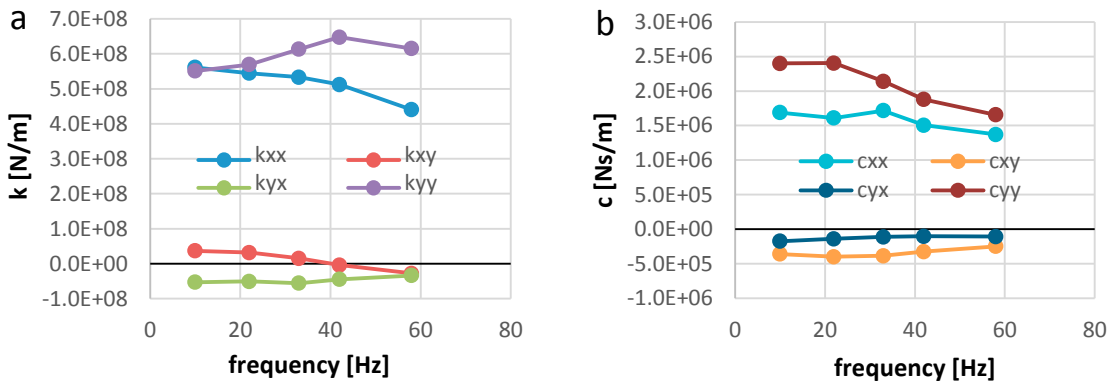

Fig. 13. Bearing (a) stiffness coefficients; (b) damping coefficients; at 3000 rpm, 58 kN static load, 4 kN per dynamic load component, 10-22-33-42-58 Hz excitation frequencies.

The synchronous data (in this case corresponding to 50 Hz) were easily calculated by interpolation. Such an operation was repeated for different rotating speeds obtaining the diagrams of Fig. 14. As expected for TPJBs, the cross-coupled coefficients are always much lower than the direct ones. Direct stiffness and damping coefficients decrease with speed. Such results were considered satisfactory with respect to the numerical results of dedicated codes.

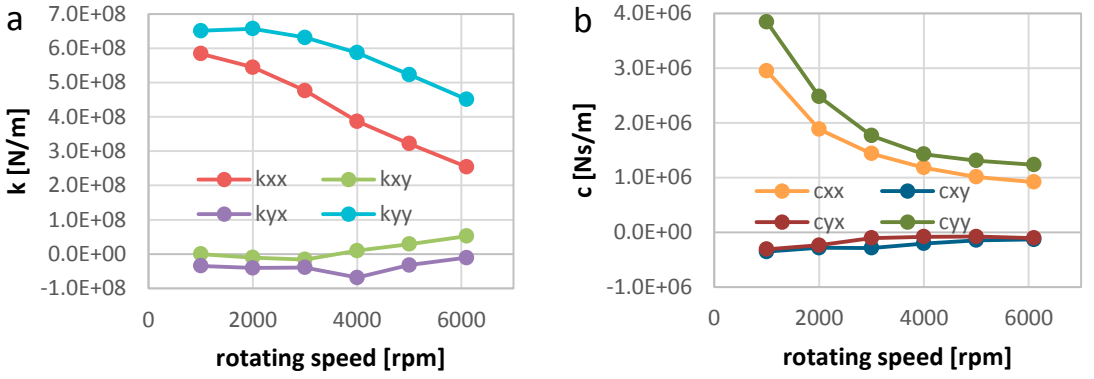

Fig. 14. Bearing dimensionless synchronous (a) stiffness coefficients; (b) damping coefficients; as function of rotating speed, for 58 kN static load.

6. Conclusions

A new test bench realized by the Department of Civil Engineering and Industrial of the University of Pisa in collaboration with BHGE and AM Testing for high performance TPJBs was presented. According to the industrial partners, the "flexibility" of the stand to test bearings with diameters from 150 to 300 mm is fundamental and innovative. The commissioning tests have demonstrated the test apparatus effectiveness in the identification of the

dynamic characteristics of large bearings. The experimental results were considered by BHGE satisfactory with respect to the numerical results of dedicated codes.

Tests are planned in the next future to investigate the effects of static load, oil temperature, and flow rate. At present, 5-pad bearing characterization tests are underway in various configurations and innovative designs.

Acknowledgements

The authors acknowledge the financial support of Tuscany Region.

References

Bang, K.B., Kim, J.H., Cho, Y.J., 2010. Comparison of power loss and pad temperature for leading edge groove tilting pad journal bearings and conventional tilting pad journal bearings. Tribology International, 43, 1287–1293.

Childs, D.W., Hale, K., 1994. A Test Apparatus and Facility to Identify the Rotordynamic Coefficients of High-Speed Hydrostatic Bearings. ASME Journal of Tribology, 116, 337–344.

Chatterton, S., Pennacchi, P., Dang P.V., Vania, A., 2014. A test rig for evaluating tilting–pad journal bearing characteristics. Proceedings of 9th international conference on rotor dynamics (IFToMM). Milan,Italy, September 22–25, 21, 921–930.

Chatterton, S., Pennacchi, P., Dang P.V., Vania, A., 2014. Identification dynamic force coefficients of a five-pad tilting pad journal bearing. Proceedings of 9th international conference on rotor dynamics (IFToMM). Milan,Italy, September 22–25, 21, 931–941.

Dang, P.V., Chatterton, S., Pennacchi, P., Vania, A., 2016. Effect of the load direction on non-nominal five-pad tilting pad journal bearings. Tribology Internationa, l98, 197–211.

Dimond, T.W., Sheth, P.N., Allaire, P.E., He, M., 2009. Identification methods and test results for tilting pad and fixed geometry journal bearing dynamic coefficients – A review. Shock and Vibration, 16, 13–43.

Dimond, T., Younan, A., Allaire, P., 2011. A review of tilting pad bearing theory. International Journal of Rotating Machinery, paper # 908469.

Forte, P., Ciulli, E., Saba, D., 2016. A novel test rig for the dynamic characterization of large size tilting pad journal bearings. Journal of Physics, Conference Series, 744, 1-12.

Ha, H.C., Yang, S.H., 1999. Excitation Frequency Effects on the Stiffness and Damping Coefficients of a Five-Pad Tilting Pad Journal Bearing. ASME Journal of Tribology, 121, 517-522.

Ikeda, K., Hirano, T., Yamashita, T., Mikami, M., Sakakida, H., 2006. An Experimental Study of Static and Dynamic Characteristics of a 580 mm (22.8 in.) Diameter Direct Lubrication Tilting Pad Journal Bearing. ASME Journal of Tribology, 128, 146-154.

Wygant, K., Flack, R.D., Barrett, L.E., 2004. Measured Performance of Tilting Pad Journal Bearings over a Range of Preload – Part. I: Static Operating Conditions. STLE Tribology Transactions, 47, 576-584.

Wygant, K., Flack, R.D., Barrett, L.E., 2004. Measured Performance of Tilting Pad Journal Bearings over a Range of Preload – Part. II: Dynamic Operating Conditions. STLE Tribology Transactions, 47, 585-593.